The American Journal of Human Genetics, Volume *95*

Supplemental Data

Neu-Laxova Syndrome Is a Heterogeneous Metabolic Disorder Caused by Defects in Enzymes of the L-Serine Biosynthesis Pathway

Rocio Acuna-Hidalgo, Denny Schanze, Ariana Kariminejad, Ann Nordgren, Mohamad Hasan Kariminejad, Peter Conner, Giedre Grigelioniene, Daniel Nilsson, Magnus Nordenskjöld, Anna Wedell, Christoph Freyer, Anna Wredenberg, Dagmar Wieczorek, Gabriele Gillessen-Kaesbach, Hülya Kayserili, Nursel Elcioglu, Siavash Ghaderi-Sohi, Payman Goodarzi, Hamidreza Setayesh, Maartje van de Vorst, Marloes Steehouwer, Rolph Pfundt, Birgit Krabichler, Cynthia Curry, Malcolm G. MacKenzie, Kym M. Boycott, Christian Gilissen, Andreas R. Janecke, Alexander Hoischen, and Martin Zenker

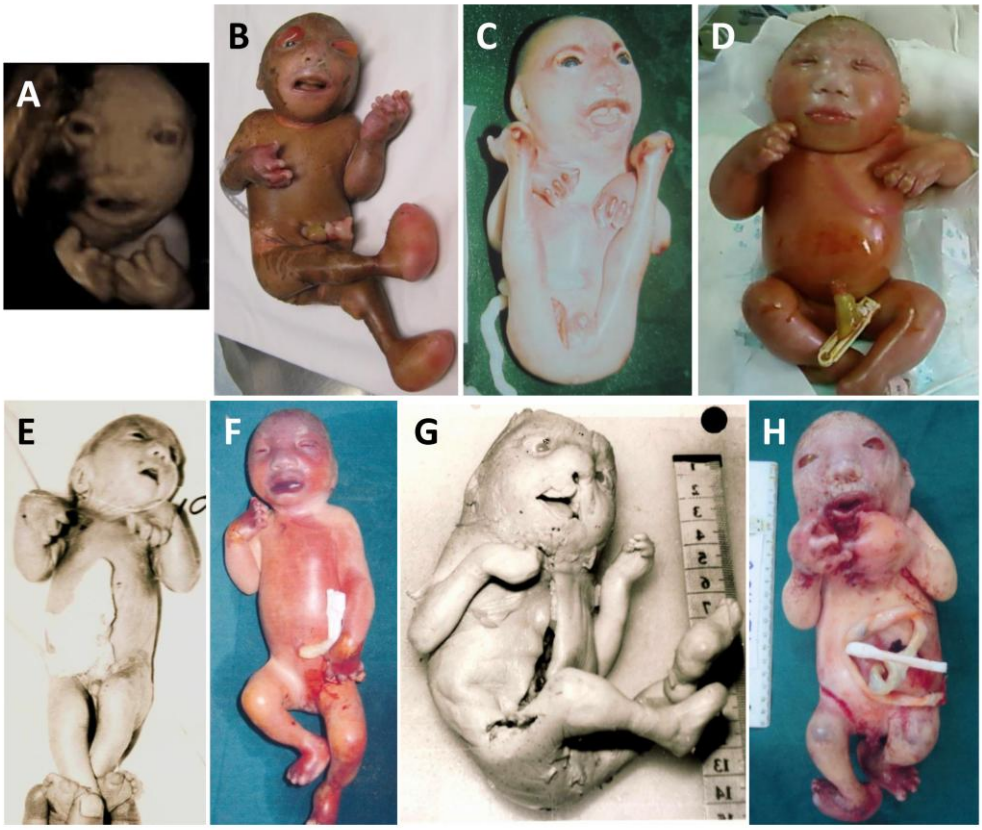

Figure S1: Clinical appearance of fetuses and newborns with NLS from this cohort

A) Prenatal 3D ultrasound at 35 weeks gestational age (GA) showing facial appearance of the affected fetus from family 1.
B) The male fetus (family 1) after termination of pregnancy at 36 weeks GA.
C) Stillborn fetus from family 3.
D) Preterm female newborn (36 weeks GA) from family 4; died in the first week of life.
E) Hypotrophic female newborn from family 5 at age 4 days; died at age 10 days.
F) Stillborn female fetus after termination of pregnancy (30 weeks GA) from family 6.
G) Stillborn fetus with cleft lip and palate from family 10.
H) Stillborn male fetus (33 weeks GA) from family 11.
Note the variability in the severity of clinical expression within this NLS cohort.

P1

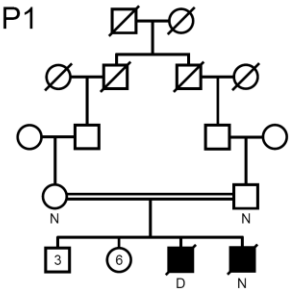

PSAT1: *c.1023_1027delinsAGACCT

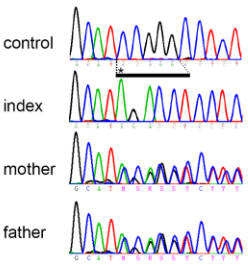

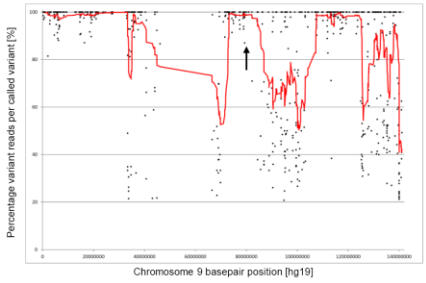

P2

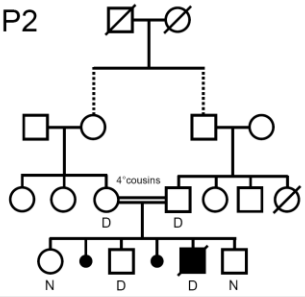

PSAT1: *c.296C>T, °c.297T>G

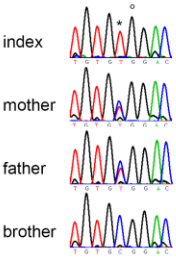

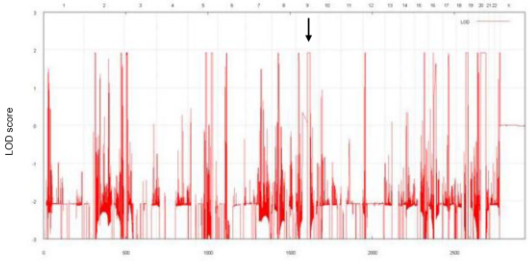

P3

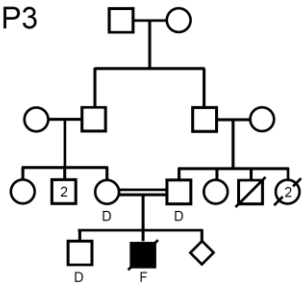

PSAT1: *c.536C>T

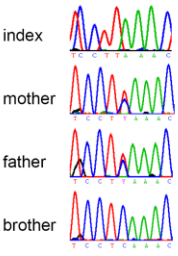

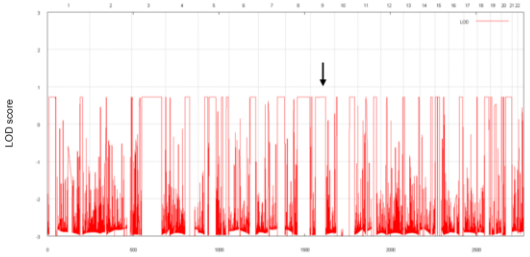

P4

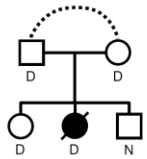

PSAT1: *c.296C>T, °c.297T>G

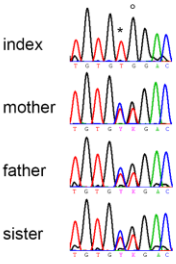

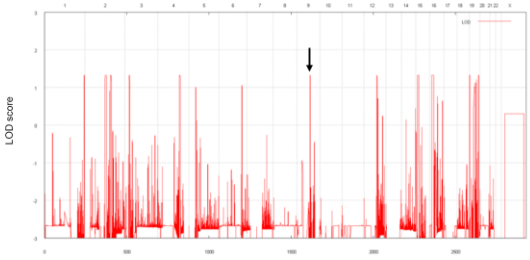

P5

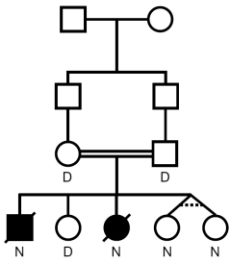

PSAT1: *c.296C>T, °c.297T>G

index n.a.

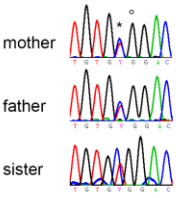

P6

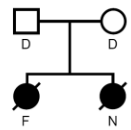

PSAT1: *c.296C>T, °c.297T>G, †c.536C>T

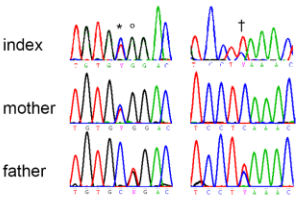

P7

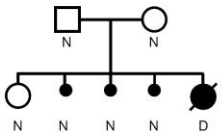

PHGDH: *c.160C>T (het)

index 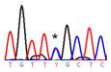

mother n.a.

father n.a.

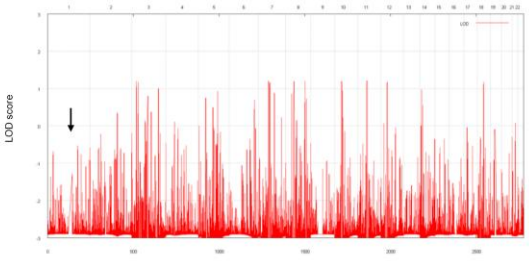

P8

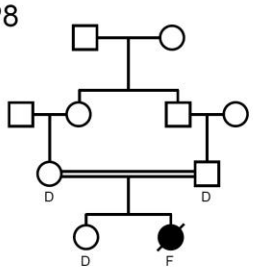

PHGDH: *c.793G>A

index 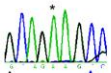

mother 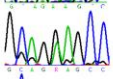

father 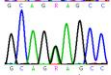

sister 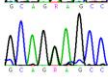

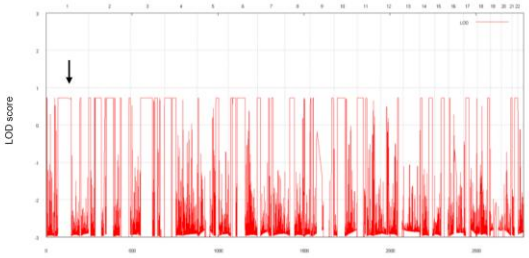

P9

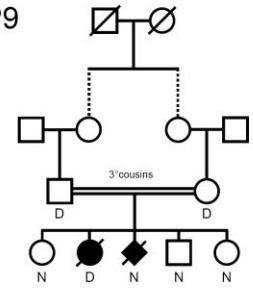

PHGDH: *c.856G>C

index 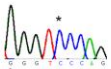

mother 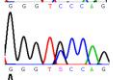

father 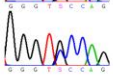

P10

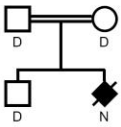

PSPH: *c.267delC

index n.a.

mother 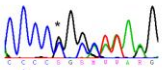

father 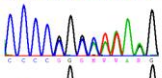

brother 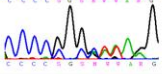

P11

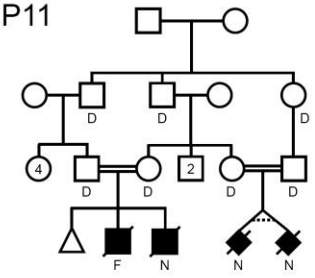

no causative mutation identified

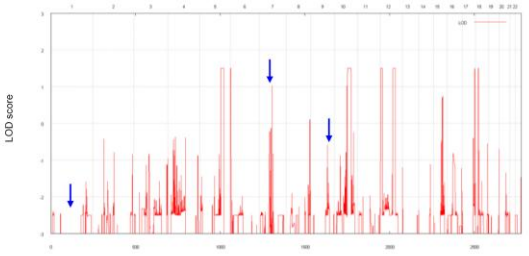

P12

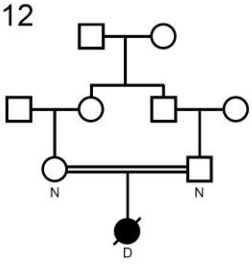

no causative mutation identified

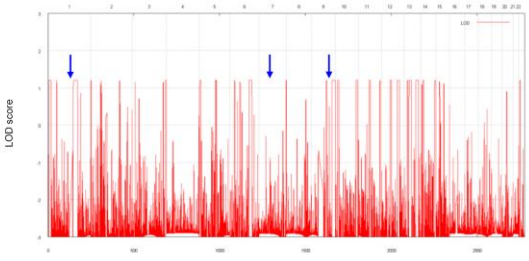

Figure S2: Pedigrees, sequencing results and homozygosity mapping in the 12 families included in this study.

In the pedigrees, "D" denotes individuals, from which DNA samples were available; "F" denotes individuals, from which only FFPE tissue material was available; "N" marks individuals from the core families, from which no material was available for this study. Numbers within circles / boxes stand for the number of healthy siblings of the respective gender. Sequence traces generated by Sanger sequencing are shown. Asterisks indicate the position of the mutation. For P1, the black bar with dashed lines marks the position of the five nucleotides deleted from the wildtype (control sequence on top shown for comparison) and six nucleotides inserted instead. In P2, P4, P5, and P6, the mutation c.296T>C (*) is adjacent to the known SNP c.297T>G (°) (dbSNP: rs3739474).

Molecular karyotyping by microarray was performed following hybridization of the patient and/or parental DNA sample to HumanCytoSNP-12v2 BeadChip high-density SNP arrays (Illumina), and according to the manufacturer's instructions. Raw SNP call data were processed with the Genotyping Analysis Module of GenomeStudio 1.6.3 (Illumina). Copy-number variants and segments of loss-of-heterozygosity (LOH) were called and visualized using PennCNV software. Multipoint LOD scores and haplotypes were obtained with the Merlin program under the hypothesis of an autosomal-recessive, fully penetrant mutation, inherited identical-by-descent. In P4, where no consanguinity was reported, this analysis could confirm at least a distant parental relationship by showing significant regions of homozygosity. In P7, no evidence of parental consanguinity was found. Exome data of family 1 were also analyzed for large homozygous regions as previously described.[1] This plot shows all high quality SNVs called in the exome analysis (black dots) sorted for their genomic positions (x-axis), plotted against the called variant read percentage (y-axis). The red line indicates an averaging window of the variant percentage of 20 consecutive variants. This identified three large homozygous stretches on chromosome 9, one of which overlaps with *PSAT1.* Arrows indicate the gene loci or *PHGDH* (chromosome 1), *PSAT1* (chromosome 9), and *PSPH* (chromosome 7), respectively. In P11 and P12, these three loci are not within the calculated homozygous regions of linkage. n.a., not available

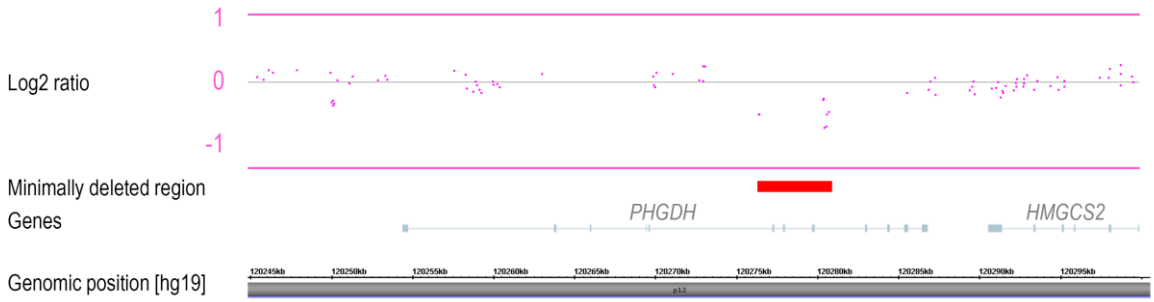

Figure S3: Heterozygous intragenic deletion of* PHGDH *detected in fetal DNA from family #7.

A CytoScanHD microarray revealed a intragenic *PHGDH* deletion, for which 8 consecutive markers reported a loss of 1 allele. The first deleted array-probe is C-3NEBO (genomic position chr1:120,276,386) the last deleted array-probe is C-3DKRL (genomic position chr1: 120,280,721). This deletion was not picked up by the initial 250k array that was used for mapping, as only 3 array probes spanned *PHGDH*. The pink squares depict the normalized log2 intensity ratio of CytoScanHD array probes based on the genomic position along chromosome 1. The red box indicates the minimally deleted region (genomic position chr1: 120,276,386-120,280,721). The grey track indicates the genes *PHGDH* and *HMGCS2* depicted in this view; the lowest track shows the genomic position on chromosome 1, based on hg19.

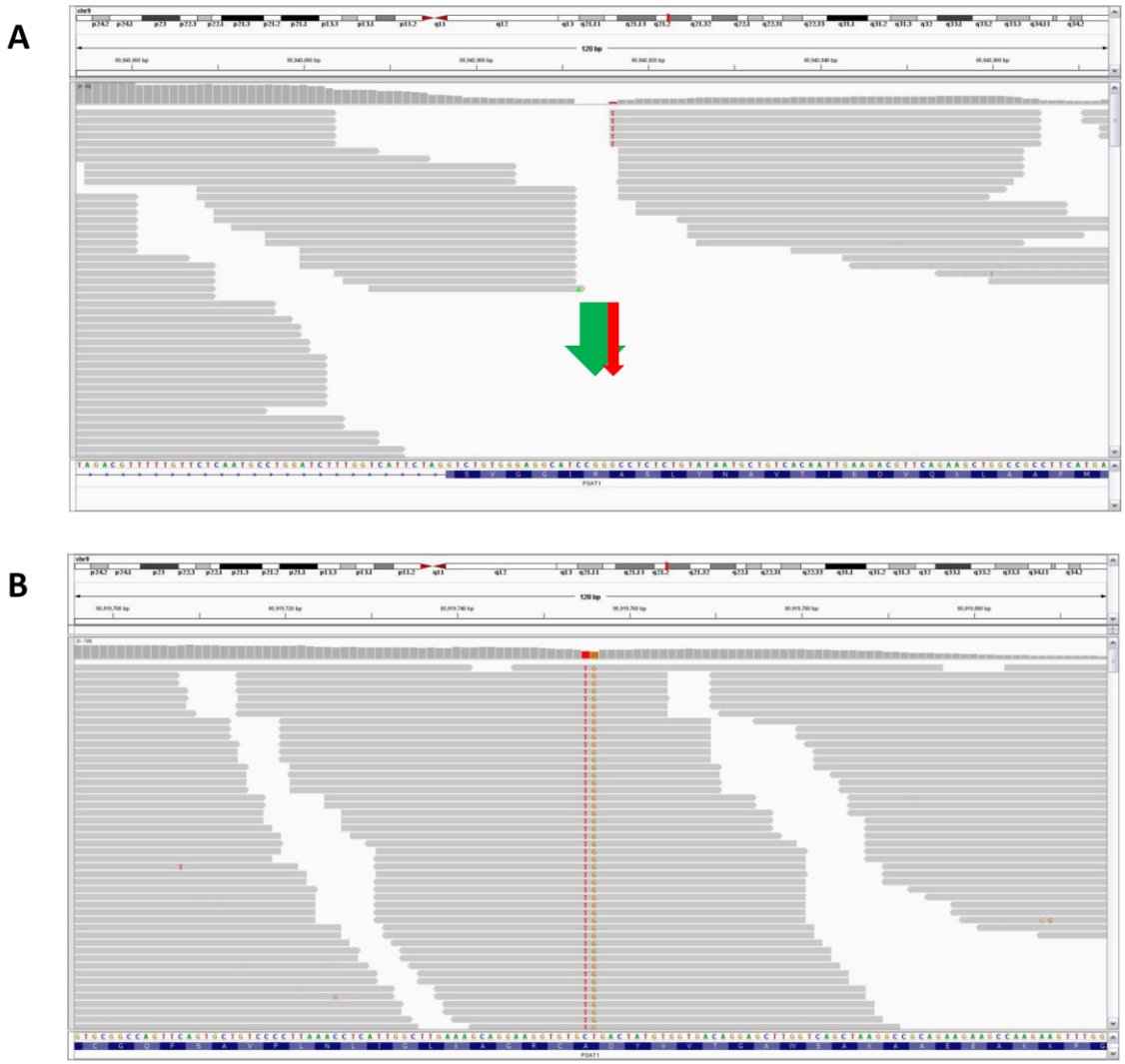

Figure S4: Screenshots of visualization of PSAT1 variants on BAM files from exome sequencing data

These two *PSAT1* mutations were initially missed by routine calling from exome sequencing. Aligned reads for proband 1 and proband 2 are shown (bam file visualized in IGV; https://www.broadinstitute.org/igv).

A) A homozygous complex insertion-deletion (c.1023_1027delinsAGACCT [p.(rg342Aspfs*6]) was identified in family 1. This complex mutation was not correctly called by initial exome sequencing; but only called as a c.1027G>T substitution (red arrow); only by manual read inspection we discovered truncated reads and missing coverage of 5 nucleotides (green arrow); indicative for a more complex event. This was finally shown by Sanger sequencing as shown in Figure S1.

B) In the index patient from family 2, we identified a homozygous missense mutation (c.296C>T [p.(Ala99Val]). Strikingly, this mutation was in direct proximity to a known SNP (rs3739474) (red arrow). This proximity of two single nucleotide substitutions prohibited calling the c.296C>T mutation from color space exome data in the first place. This mutation was only called by re-analysis using GATK variant calling (https://www.broadinstitute.org/gatk) and was clearly visible upon manual read inspection. The routine exome sequencing was performed by using Agilent's SureSelect exome enrichment ((v2 or v4 respectively, Agilent, Santa Clara, USA) in combination with SOLiD sequencing (SOliD4 or 5500xl respectively, Life Technologies, Foster City, USA) as previously described.[1–3] Lifescope (Life Technologies, Foster City, USA) and GATK software were used for variant calling and variant annotation, filtering and prioritization was performed as described previously.[1,4]

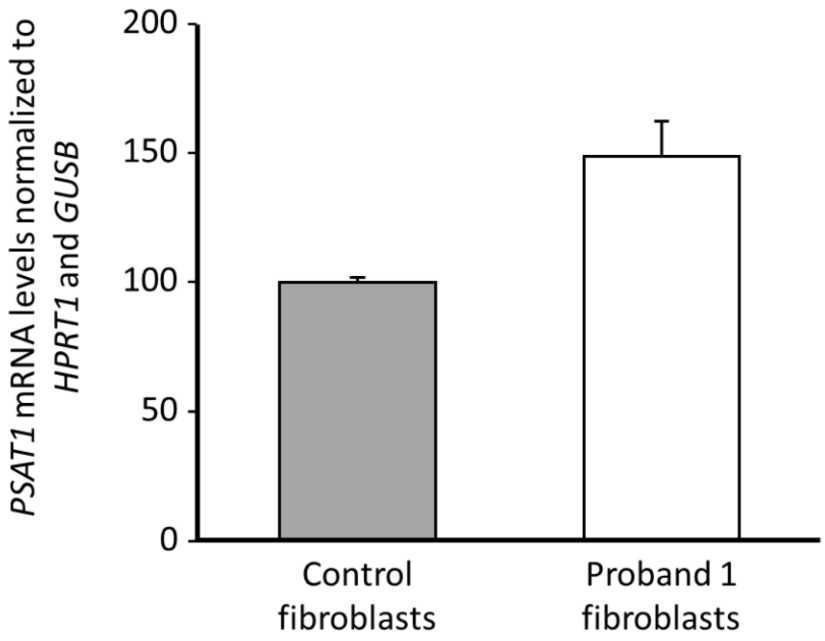

Figure S5: mRNA levels of PSAT1 in fetus with homozygous frameshift mutation in PSAT1

Results from qPCR showing levels of *PSAT1* mRNA in fibroblasts from the fetus from family 1, compared to fibroblasts from a fetus of a similar gestational age and normalized to *HRPT1* and *GUSB*. Bars represent the standard error. Fetal fibroblasts were cultured and mRNA was extracted using the RNeasy kit (Qiagen, Hilden, Germany). Purified RNA was quantified, normalized and an RT-PCR was performed with Superscript III Reverse transcriptase (Life Technologies). GoTaq SYBR green qPCR master mix was used in the qPCR reaction which was run on a 7900HT Fast real time PCR system (Applied Biosystems). Primer sequences are available upon request.

Table S1: Summary of phenotypic characteristics of our cohort of NLS patients

	Pt1	Pt2	Pt3	Pt4	Pt5	Pt6	Pt7	Pt8	Pt9	Pt10	Pt11	Pt12	Summary [n]	Summary [%]	Literature comparison[a]
Genetics															
Affected gene	*PSAT1*	*PSAT1*	*PSAT1*	*PSAT1*	*PSAT1*	*PSAT1*	*PHGDH*	*PHGDH*	*PHGDH*	*PSPH*	-	-			
Mutation at protein level	Arg342Aspfs*6	Ala99Val	Ser179Leu	Ala99Val	Ala99Val	Ala99Val/ Ser179Leu	Arg54Cys/ del	Glu265Lys	Ala286Pro	Gly90Alafs*2	NA	NA			
Cranium/face															
Slanted forehead	**1**	**1**	**1**	**1**	**1**	**1**	**NA**	**1**	**1**	**1**	**1**	**1**	**11/11**	**100%**	**50 [2]**
Hypertelorism	1	1	0	0	1	1	1	1	1	0	1	1	9/12	75%	37 [0]
Proptosis	1	1	1	0	1	0	1	0	1	1	1	1	9/12	75%	37 [2]
Cataract	NA	0	NA	NA	NA	0	1	0	1	0	NA	0	2/7	29%	2 [0]
Absent of abnormal eyelids	1	1	1	0	1	0	1	1	1	1	1	0	9/12	75%	26 [1]
Lowset or malformed ears	**1**	**1**	**1**	**1**	**1**	**1**	**1**	**0**	**1**	**1**	**1**	**1**	**11/12**	**92%**	**42 [2]**
Flat or abnormal nose	**1**	**1**	**1**	**1**	**1**	**1**	**1**	**1**	**1**	**1**	**1**	**1**	**12/12**	**100%**	**48 [3]**
Micrognathia	**1**	**1**	**1**	**1**	**1**	**1**	**1**	**1**	**1**	**1**	**1**	**1**	**12/12**	**100%**	**38 [1]**
Cleft palate and/or palate	1	0	0	0	0	0	1	0	0	1	0	0	3/12	25%	16 [1]
Abnormal mouth	**1**	**1**	**1**	**1**	**1**	**1**	**1**	**0**	**1**	**1**	**1**	**1**	**11/12**	**92%**	**16 [0]**
Round gaping mouth	1	1	1	1	1	0	1	0	1	0	1	0	8/12	67%	4 [1]
CNS															
Prominent occiput	0	0	0	0	0	0	0	0	0	0	0	0	0/12	0%	2 [0]
Microcephaly	**1**	**1**	**1**	**1**	**1**	**1**	**1**	**1**	**1**	**1**	**1**	**1**	**12/12**	**100%**	**59 [3]**
Lissencephaly	NA	NA	NA	1	NA	0	0	1	N/A	0	1	0	3/7	43%	29 [0]
Hypoplastic/abnormal cerebellum	NA	NA	NA	NA	NA	NA	1	1	1	0	0	0	3/6	50%	26 [0]
Agenesis/abnormal corpus callosum	NA	NA	NA	NA	NA	NA	0	1	N/A	0	1	1	3/5	60%	22 [0]
Decreased/absent gyri	NA	NA	1	1	NA	0	0	1	N/A	0	1	NA	4/7	57%	12 [1]
Dilated/abnormal ventricles	NA	NA	NA	NA	NA	NA	0	0	N/A	1	0	1	2/5	40%	17 [1]
Calcifications	NA	NA	NA	NA	NA	NA	1	0	N/A	0	0	0	1/5	20%	4 [0]
Spina bifida	0	0	0	0	NA	0	1	0	0	0	0	0	1/11	9%	2 [0]
Limbs															
Deformity of digits	**1**	**1**	**1**	**1**	**1**	**1**	**1**	**1**	**1**	**1**	**1**	**0**	**11/12**	**92%**	**45 [2]**
Deformity of limbs	**1**	**1**	**1**	**1**	**1**	**1**	**1**	**1**	**1**	**1**	**1**	**1**	**12/12**	**100%**	**33 [2]**
Flexion deformity	**1**	**1**	**1**	**1**	**1**	**1**	**1**	**1**	**1**	**1**	**1**	**0**	**11/12**	**92%**	**51 [2]**
Syndactyly fingers	1	0	0	0	0	0	1	0	1	0	1	0	3/12	25%	18 [0]
Syndactyly toes	1	0	0	0	0	0	1	1	1	1	1	1	7/12	58%	13 [0]
Rockerbottom feet	**1**	**1**	**1**	**1**	**1**	**1**	**1**	**1**	**1**	**1**	**1**	**1**	**12/12**	**100%**	**31 [1]**
Swollen hands or feet	**1**	**1**	**1**	**1**	**1**	**1**	**1**	**1**	**1**	**1**	**1**	**0**	**11/12**	**92%**	**5 [1]**
Other															
IUGR	**1**	**1**	**1**	**1**	**1**	**1**	**1**	**1**	**1**	**1**	**1**	**1**	**12/12**	**100%**	**53 [1]**
Short neck	**1**	**1**	**1**	**1**	**1**	**1**	**1**	**1**	**1**	**1**	**1**	**0**	**11/12**	**92%**	**46 [3]**
Subcutaneous edema	1	1	0	1	0	1	NA	1	1	1	1	0	8/11	73%	48 [2]
Ichthyosis/taut skin	**1**	**1**	**1**	**1**	**1**	**1**	**1**	**1**	**1**	**1**	**1**	**1**	**12/12**	**100%**	**47 [2]**
Hypoplastic/atelectatic lungs	1	NA	1	0	0	0	0	1	N/A	0	1	0	4/10	40%	17 [0]
Ambiguous/hypoplastic genitalia	1	0	1	0	0	0	0	0	1	1	1	0	5/12	42%	29 [0]
Short umbilical cord	NA	NA	NA	NA	NA	0	NA	NA	N/A	NA	0	0	0/3	0%	14 [0]
Polyhydramnios	1	0	NA	NA	NA	0	1	NA	0	1	0	0	3/8	38%	26 [1]
Wide-spaced nipples	NA	NA	NA	NA	0	0	NA	1	1	1	0	0	3/7	43%	6 [0]
Protruding abdomen	0	0	0	0	0	0	0	0	1	0	0	0	1/12	8%	1 [0]
Heart defect	NA	0	0	NA	NA	0	0	0	N/A	0	0	0	0/8	0%	3 [0]
Consanguinity	1	1	1	1	1	0	0	1	1	1	1	1	10/12	83%	32 [3]
Decreased or absent fetal movements	**1**	**1**	**NA**	**1**	**NA**	**1**	**NA**	**1**	**1**	**NA**	**NA**	**1**	**7/7**	**100%**	**5 [1]**
Scoliosis	1	0	1	0	0	0	0	0	1	0	0	0	3/12	25%	13 [0]
Other spine alterations	NA	0	0	0	0	0	0	0	N/A	0	0	0	0/10	0%	3 [1]
Other observations	'Snow storm appearance' of the amniotic fluid; cryptorchidism			Liveborn, died in the first week of life	Liveborn, died at age 10 days	High palate		High palate		Wide fontanel; mild hypoplastic female genitalia	High palate; hypoplastic scrotum	Arachnoid cyst; survived 2 months; suspected dysplastic kidneys; hypothyroidism; exocrine pancreatic insufficiency			

[a] Modified from Manning *et al*[5]. and based on 70 cases with NLS from literature[6–12]. Clinical information from the previous report of Shaheen *et al.* is shown between brackets. Only cases for which the phenotype was reported are counted here. 1 present; 0 not present; NA not analyzed. All features that are present in >90% of our cases are printed in bold.

Supplemental References

1. Stránecký, V., Hoischen, A., Hartmannová, H., Zaki, M.S., Chaudhary, A., Zudaire, E., Nosková, L., Barešová, V., Přistoupilová, A., Hodaňová, K., et al. (2013). Mutations in ANTXR1 cause GAPO syndrome. Am. J. Hum. Genet. *92*, 792–799.

2. Hoischen, A., van Bon, B.W.M., Rodríguez-Santiago, B., Gilissen, C., Vissers, L.E.L.M., de Vries, P., Janssen, I., van Lier, B., Hastings, R., Smithson, S.F., et al. (2011). De novo nonsense mutations in ASXL1 cause Bohring-Opitz syndrome. Nat. Genet. *43*, 729–731.

3. Hoischen, A., van Bon, B.W.M., Gilissen, C., Arts, P., van Lier, B., Steehouwer, M., de Vries, P., de Reuver, R., Wieskamp, N., Mortier, G., et al. (2010). De novo mutations of SETBP1 cause Schinzel-Giedion syndrome. Nat. Genet. *42*, 483–485.

4. Gilissen, C., Arts, H.H., Hoischen, A., Spruijt, L., Mans, D. a, Arts, P., van Lier, B., Steehouwer, M., van Reeuwijk, J., Kant, S.G., et al. (2010). Exome sequencing identifies WDR35 variants involved in Sensenbrenner syndrome. Am. J. Hum. Genet. *87*, 418–423.

5. Manning, M.A., Cunniff, C.M., Colby, C.E., El-Sayed, Y.Y., and Hoyme, H.E. (2004). Neu-Laxova syndrome: detailed prenatal diagnostic and post-mortem findings and literature review. Am. J. Med. Genet. A *125A*, 240–249.

6. Mihci, E., Simsek, M., Mendilcioglu, I., Tacoy, S., and Karaveli, S. (2005). Evaluation of a fetus with Neu-Laxova syndrome through prenatal, clinical, and pathological findings. Fetal Diagn. Ther. *20*, 167–170.

7. Martín, A., Eguiluz, I., Barber, M. a, Medina, N., Plasencia, W., García-Alix, A., and García-Hernández, J. a (2006). A rare cause of polyhydramnios: Neu-Laxova syndrome. J. Matern. Fetal. Neonatal Med. *19*, 439–442.

8. Ugras, M., Kocak, G., and Ozcan, H. (2006). Neu-Laxova syndrome: a case report and review of the literature. J. Eur. Acad. Dermatol. Venereol. *20*, 1126–1128.

9. Kahyaoglu, S., Turgay, I., Ertas, I.E., Ceylaner, S., and Danisman, N. (2007). Neu-Laxova syndrome, grossly appearing normal on 20 weeks ultrasonographic scan, that manifested late in pregnancy: a case report. Arch. Gynecol. Obstet. *276*, 367–370.

10. Tarim, E., and Bolat, F. (2010). Prenatal diagnosis and postmortem findings of Neu-laxova syndrome. J. Turkish Ger. Gynecol. Assoc. *11*, 225–227.

11. Manar, A.-L., and Asma, B. (2010). Neu-Laxova syndrome: A new patient with detailed antenatal and post-natal findings. Am. J. Med. Genet. A *152A*, 3193–3196.

12. Shaheen, R., Rahbeeni, Z., Alhashem, A., Faqeih, E., Zhao, Q., Xiong, Y., Almoisheer, A., Al-Qattan, S.M., Almadani, H. a, Al-Onazi, N., et al. (2014). Neu-Laxova Syndrome, an Inborn Error of Serine Metabolism, Is Caused by Mutations in PHGDH. Am. J. Hum. Genet. *94*, 898–904.